The Out-reactor Performance of New Zirconium Alloys

Jing Zhou(SNZ)[1], Lian Wang[1], Gang L[1]i, Bo Gao[1], Sheng Peng[1],
Liutao Chen[2], Jun Tan[2], Hong Zou[2],Rui Li[2], Dungu Wen[2] Baoxin Zhou[2],Meiyi Yao[2]
1. SNZ, Baoji, Shaanxi 721013, P. R. China
2. China Nuclear Power Technology Research Institute, Shenzhen of Guangdong Prov.518026,China
Corresponding author: mulle @163.com

New zirconium alloys (SZA-1, SZA-3, SZA-4, SZA-6) cladding tubes were introduced and plenty of out-reactor experiments were performed to develop a further understanding of the relationship between alloy chemistry, microstructure and mechanical properties, corrosion performance. The results show that SZA-4,SZA-6 were not completely re-crystallized, while SZA-1, SZA-3 and Zirlo were re-crystallized completely after heat treatment for 560℃/3h. Tensile test results show that (SZA-1,SZA-3)＜(SZA-4, SZA-6) ＜Zirlo, Hydrogen pickup and CSR of the four cladding tubes were quite the same as Zirlo cladding tube. Corrosion test results indicate that, these four zirconium alloys show the same corrosion resistance as Zirlo at 400℃, 10.3MPa for 72h. Long term corrosion test shows that these four zirconium alloys have better corrosion performance than Zirlo.

Application of the BP Network Technology Improved by Genetic Algorithm in the Optimization of Cladding Tubes' Flooding-focused Ultrasonic Detection Parameters

Lin H. Chu[1], Hai L. Wang[1], Chun Q. Hu[2], Lian Wang[1], Gai H. Yuan[1] and Xiao S. Li[1]
1. State nuclear BaoTi Zirconium industry Company, Shanxi, Baoji, 721003, P. R. China
2. Institute of Metal Research of Chinese Academy of Sciences, Liaoning, Shenyang, 110016
*Corresponding author: chulinhuascu@163.com

Based on the special applied environment, the quality inspection problems of Zirconium alloy cladding tubes can't be ignored. For a long time, the flooding-focused ultrasonic wave detection techniques were used to examine a variety of manufacturing defects and control the cladding tubes' quality. However, due to the small diameter and thin thickness, the tubes' sizes is very close to the limit of ultrasonic flooding-focused detection. While not grasping the precise detection parameters in the actual ultrasonic testing process, it is prone to the wrong judgment and undetected cases to the tubes' defects, and forming the significant security risks. Therefore, in order to improve the accuracy of ultrasonic testing and reduce the defects' wrong judgment ratio, it is necessary to optimize and design the main testing parameters systematically.

Many studies have improved that, the artificial neural network technology is a kind of powerful and effective assistant tool to the optimization and analysis of various engineering problems. And the error back-propagation neural network (BPNN) is one of the most successful and widely applied styles. For the ultrasonic testing process, it can be used to train and build a precise BPNN prediction model between the test parameters and results. With the model, it is easy to obtain a set of optimized testing parameters, and then achieve the goal of improving the accuracy and reliability in the cladding tubes' defects testing.

In this paper, in order to optimize the ultrasonic testing parameters, an improved GA-BP prediction model based on the genetic algorithms (GA) had been tried to build. And the superiority of new model compared with the common BP model was studied mainly. Before the model's training, for reducing model's scale, SAS software was used to finish the significant analysis of various testing parameters, and screened out four main factors finally: guide sleeve's gap, feeding speed, repeated frequency and selected speed. Then, taking the four testing parameters as the input variables and echo amplitude as the output variable, two 4-6-1 GA-BP models of some kind small tubes' inner and outer defects were trained and built respectively with MATLAB software. It is worth pointing out that the adaptive genetic algorithm was especially used here to search the global optimal weights and thresholds, and prevent the normal BP network from falling into the local minimization. The main training parameters are follows: evolving times 50, size of population 30, crossed probability 0.3, probability of mutation 0.1 and the fitness function chosen according to the targets' error.

The results show that, on the one hand, all prediction error values given by the different models are within the range of required accuracy. On the other hand, whether predict accuracy or constringency speed, there are significant differences in the different models. For the inner injuries' model, the echo amplitude's maximum relative error predicted by normal BP method is nearly 12.6%, and training steps 123. However, the maximum error is only 6.5% for the GA-BP model which converged in the step 43. Tubes' outer model has the same compared results. The ordinary BP model predicts the maximum error values as high as 13.8%, while the GA-BP optimization model is less than 7%. Meanwhile, the latter also can finish the operating process faster. It can be concluded that, the new GA-BP network technology has not only overcome the local minima defects of normal BP algorithm, but also improved the local searching capability of genetic algorithm. It will be more suitable for the optimization study of ultrasonic testing parameters.

Stress-reorientation of Hydrides in N36 Zirconium Alloy Cladding Tube

Xie Meng[1,2], Chen Le[1] ,Dai Xun[1], Xu Chunrong[1],Chen Shanhua[2]

(1 National Key Laboratory for Nuclear Fuel and Materials, Nuclear Power Institute of China,Chengdu610041;

2 Chengdu University of Technology,Chengdu610059)

Abstract

During the nuclear power reactor operation, the oxidation and subsequent hydrogen absorption for the fuel elements cladding would be caused by a waterside corrosion ,which decreased the initial ductility of the zirconium alloy cladding. The extent of cladding embrittlement depends not only on the quantity of hydride but also on its morphology and in particular the orientation of hydrides with respect to the applied stress. Metallographic microscope with processing system was used to analysis the morphology and orientation factor of hydrides in N36 zirconium alloy tube. Under the different circumferential tensile stress and thermal cycling between 200 to 400℃, the effects of stress and the time of thermal cycling on the reorientation of hydrides in N36 tubes specimen containing 200 to 300 ppm hydrogen were investigated. The radial hydrides could be formed by the reorientation process, when the specimen was cooled down under the stress above threshold stress from 400℃ at which hydrides were dissolved. The results showed that some of hydrides changed from the circumferential to the radial distribution and the hydride orientation factor(F_N^{30}) increased with increasing the time of thermal cycling.When the hydrides reorientation became more noticeable, the radial hydrides became the thicker and longer. In once and twice thermal cycling, the stress-reorientation of hydrides had happened under a hoop stress of 95 MPa and 50 MPa, respectively.The nonuniformity of the morphology and distribution of hydrides was reflected in the different samples under the same conditions, the different field of the same sample and in the inner, the middle and the outer layer of the same field of view. The detailed analysis shows that the stress-reorientation of hydrides was not only related with the temperature and stress, but also related to the texture, grain size and residual stress. Therefore, further study should be carried out to understand the mechanism and regularity of the hydride orientation happened in N36 zirconium alloy cladding tube.

Keywords: N36 zirconium alloy, cladding tube, hydrides reorientation

? high cooling rate 100°C/h

3.2 Effect of hoop St. on reorientation ?

Conclusion 2

Separation efficiency of impurities from Zirconium scrap by electrorefining with electrolyte composition

Seung Hyun Kim[1], Dong Jae Park[1], Hui Li[1], Jong Hyeon Lee[1,2,*]

Graduate School of Green Energy Technology in Chungnam national university, 79 Daehak-ro, Yuseong-gu, Daejeon 305-764, Republic of Korea[1]

Department of NanoMaterials Engineering, Chungnam National University, 79 Daehak-ro, Yuseong-gu, Daejeon 305-764, Republic of Korea[2]

Generation of unradiated Zirconium scrap in Korea will reach 500 tons/year in 2018 as the new nuclear power plants are deployed. If this Zirconium scrap is recycled, it can be turned into high value-added strategic resources. There are a number of ways to recycle zirconium scrap, wet and dry processes. The dry process is known as more simple compared to wet chemical process because it utilizes the method that doesn't need toxic chemical chlorine gas and conversion step. Hence, electrorefining process as a representative dry process was used in this study to recover pure Zirconium from nucrear grade zirconium scrap. The effect of molten salt composition with fluorine and chlorine ratio in LiF-KF molten salt was studied on the separation efficiency and microstructure of deposit. Electrochemical tests such as cyclic voltammetry and chrono potentiometry were performed depending on addition of 1, 5, and 10wt% of LiCl-KCl to the based molten salt. It was also used ICP analysis in order to measure electrodeposit composition. The microstructure, crystal structure and thermal characteristics of electrodeposit were assessed multilaterally by SEM, XRD and TGA respectively.

The Characterizations of SZA-6 Strip and Tube

Gang Li[1], Sheng Peng[1], Lian Wang[1], Gaihuan Yuan[1], Qifeng Zeng[2], Jinhua Huang[2], Libing Zhu[2], Jiazheng Liu[2], Bangxin Zhou[3], Meiyi Yao[3];

(1 State Nuclear Baoti Zirconium Industry Company , Baoji, Shaanxi, China 721013;
2 Shanghai Nuclear Engineering Research and Design Insititue, Shanghai, China, 200233;
3 Insittute of Materials, Shanghai University, Shanghai, China, 200072)
Corresponding author: llkkjj11@163.com

From Zr-2 and Zr-4 developed in the early time to Zr-1% Nb(E110), E635, HANA-6, NDA and Zirlo developed recently, new zircaloys are successively applied to the commercial nuclear reactors.However, there is still no commercial zircaloy with our own independent intellectual property in China. The researchers devote to the development of the new zircaloy material with independent intellectual property in China. For example, N18 and N36 alloys are developed by Chinese Nuclear Power R&D Institute with Shanghai University; SZA 1 and 3 alloys are researched by China Nuclear Power technology Research Institute; SZA 4 and 6 alloys are studied by State Nuclear Baoti Zirconium Industry Company with Shanghai Nuclear Engineering Research and Design Insititue and Shanghai University.

The nominal composition of SZA 6 is Zr-Sn-Nb-Fe-Si. The strip and tube are manufacture by SNZ. Mechanical Properties are shown in Table 1. The mechanical properties are comparable with those of Zr-4. SEM pictures are in Figure 1. The SPPs exhibit spherical or ellipsoidal shapes. Few SPPs more than 300nm are observed in the strip and tube samples. Most SPPs are less than 100nm, and few SPPs are more than 300nm in the strip; Most SPPS are around 230nm, and a few SPPs are more than 350nm in the tube. The corrosion resistance property of SZA 6 is better than that of Zr-4 in the condition of 0.01 M LiOH solution at 360°C; but SZA 6 is worse than Zr-4 in the condition of water corrosion at 360°C; SZA 6 is comparable to Zr-4 in the condition of stream corrosion at 400 °C. One reason is that the SPPs are much bigger than Zirlo or Zr-4 SPPs; another reason is the precipitates of Lavas phase particles $Zr(Nb,Fe)_2$ in the matrix.

Table 1 Room Temperature Mechanical Properties of SZA 6

Type	Yield Strength	Ultimate Strength	Elongation
δ 0.7 mm Strip	346 MPa	446 MPa	36%
Φ 9.5mm Tube	622 MPa	827 MPa	16%

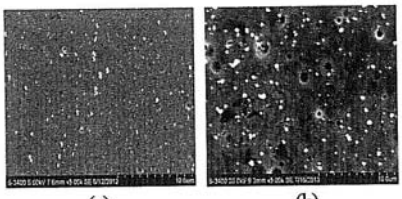

(a) (b)

Figure 1 SEM Pictures of SZA 6 Strip (a) and Tube (b)

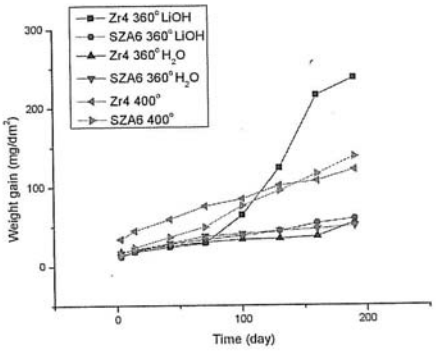

Figure 2 Corrosion Results of Zr-4 and SZA6 Strips

EFFECT OF INITIAL TEXTURE ON DEFORMATION MECHANISMS AND DYNAMIC RECRYSTALLIZATION IN ZIRCONIUM ALLOY DURING UNIAXIAL COMPRESSION

Xinyi Li, Baifeng Luan*, Qing Liu

College of Materials Science and Engineering, Chongqing University, Chongqing, 400044, P. R. China

Corresponding author: bfluan@cqu.edu.cn

In order to investigate the effect of initial texture on deformation mechanisms and dynamic recrystallization during hot compression, Zr–1Sn–0.3Nb (N18) alloy sheet with bimodal basal texture was cut into cylinder samples and make their compression axes (CA) tilt 0°, 30°, 60° and 90° to the normal direction (ND) of the sheet respectively. Uniaxial compression was performed at 650℃ with strain rates $5s^{-1}$ and $0.001s^{-1}$ by Gleeble 1500D thermo-mechanical simulation machine. The microstructure of the deformed samples was characterized using the electron backscattered diffraction (EBSD) technique. The results show that the yield strength dropped with increasing of the initial orientation in both strain rate. The yield strength of samples compressed at the strain rate of $5s^{-1}$ was approximately 2 times that for samples with strain rate of $0.001s^{-1}$. The strength drop is mainly attributed to a gradual increase of schmid factor (SF) for prismatic slip. During the compression, $\{10\bar{1}2\}$ twinning and $\{10\bar{1}1\}$ twinning were found. $\{10\bar{1}2\}$ twinning increase with the increasing of the angle with ND direction in both strain rate, while $\{10\bar{1}1\}$ twinning mainly occurred in samples that the c-axis of most grains parallel to CA at the strain rate of $5s^{-1}$. As the compression strain accumulates, dynamic recrystallization is found to occur in all specimens which show the same bimodal basal texture. In addition, a strong effect of the initial orientation on suppressing the dynamic recrystallization is revealed and the reason is attributed to the different stored energy caused by dislocation motion and twinning

Keywords: Zirconium alloy, initial texture, deformation mechanisms, dynamic recrystallization

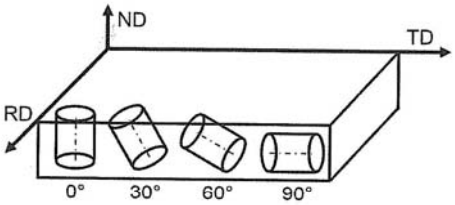

Fig. 1 Schematic illustration of the four samples used for compression testing

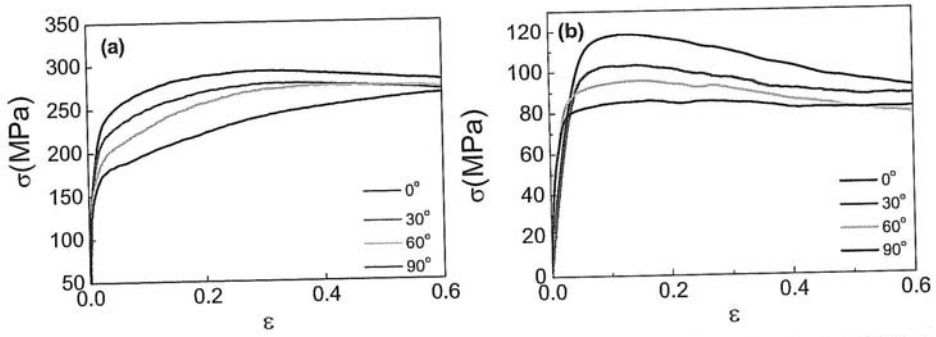

Fig. 2 Stress-true strain curves for compression at 650℃ for samples with different angles to ND: (a) strain rate 5 s^{-1} (b) strain rate 0.001s^{-1}

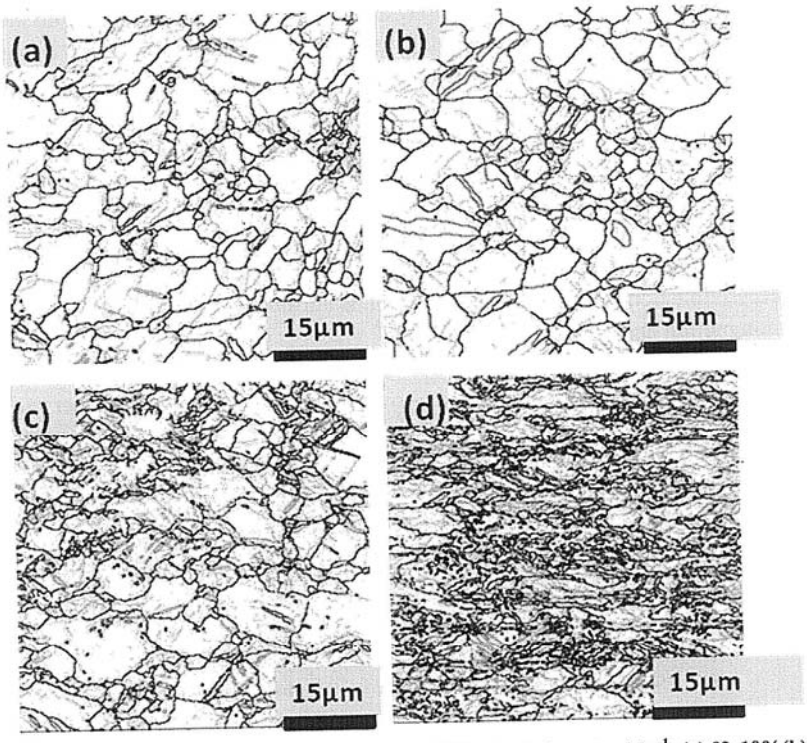

Fig. 3. Microstructures of specimens after compression at 650°C with strain rate of 5 s^{-1}: (a) 0°, 10%(b) 90°, 10% (c) 0°, 30% (d) 90°,30%. Grey, black, red and green lines indicate boundaries of low angle (2~15°), high angle (□15°), $\{10\bar{1}2\}<10\bar{1}1>$ twin and $\{10\bar{1}1\}<10\bar{1}2>$ twin, respectively.

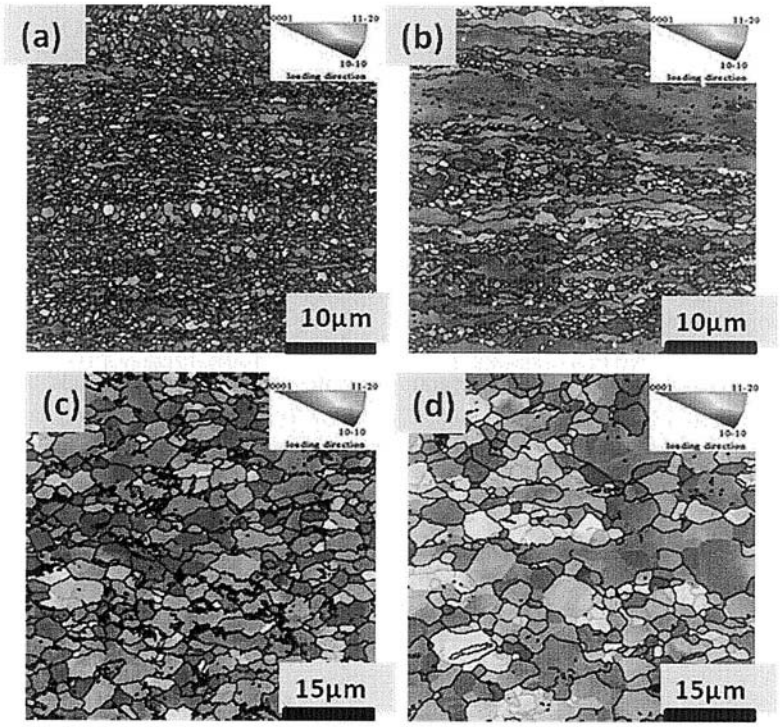

Fig.4. EBSD IPF maps of samples compressed 60%, 650℃: (a) 0°, strain rate 5 s^{-1} (b) 90°, strain rate 5 s^{-1},(c) 0°, strain rate 0.001 s^{-1},(d) 90°, strain rate 0.001s^{-1}

References

[1] Murty K, Charit I. Texture development and anisotropic deformation of zircaloys. Prog Nucl Energ 2006;48:325–59 292

[2] Chai L, Luan B, Murty KL, et al. Effect of predeformation on microstructural evolution of a Zr alloy during 550–700℃ aging after βquenching. Acta Mater 2013;61:3099–109.

[3] Akhtar A, Teghtsoonian A. Plastic deformation of zirconium single crystals. Acta Metall 1971;19:655–63.

[4] Tenckhoff E. The development of the deformation texture in zirconium during rolling in sequential passes. Metall Trans A 1978;9:1401–12.

[5] Wang B, Xin R, Huang G, and Liu Q. Effect of crystal orientation on the mechanical properties and strain hardening behavior of magnesium alloy AZ31 during uniaxial compression. Mater Sci Eng A 2012;534:588-93.

[6] Wang M, Xin R, Wang B, and Liu Q. Effect of initial texture on dynamic recrystallization of AZ31 Mg alloy during hot rolling. Mater Sci Eng A 2011;528:2941-51

[7] Akhtar A. Compression of zirconium single crystals parallel to c -axis. J Nucl Mater 1973;47:79–86. [8 Pérez-Prado MT, Barrabes SR, Kassner ME, et al. Dynamic restoration mechanisms in a-zirconium at elevated temperatures. Acta Mater 2005;53:581–91.

STUDY OF THE SZA-6 NEW ZIRCONIUM ALLOY

Qifeng Zeng*, Jinhua Huang, Libing Zhu, Jiazheng liu

Department of Reactor Core Design, Shanghai Nuclear Engineering Research and Design Institute, Shanghai 200233, China

Based on the investigation of alloying elements' effect, we designed a new zirconium alloy called SZA-6 alloy. Its composition is Zr-Sn-Nb-Fe-Si. In the stage of button, SZA-6 alloy has better corrosion resistance than ZIRLO and Zr-4 in deionized water or lithiated water with 0.01M LiOH at 360℃/18.6MPa. In the stage of small ingot, SZA-6 alloy has better or bad corrosion than ZIRLO and Zr-4 in deionized water or lithiated water with 0.01M LiOH at 360℃/18.6MPa, which depends on the heat treatment process. When the intermediate anneal of SZA-6 alloy was replaced by β-quenching, cold rolling and high temperature aging, there are several kinds of second phase particles in the alloy, $Zr(NbFe)_2$ precipitates, Zr_5Si_4 precipitates, β-Zr precipitates, $(ZrNb)_2Fe$ precipitates and Zr_3Fe precipitates. Because the existence of β-Zr precipitates, the corrosion resistance of SZA-6 alloy was very bad. In the mechanical tests, SZA-6 alloy has compared mechanical property with Zr-4.

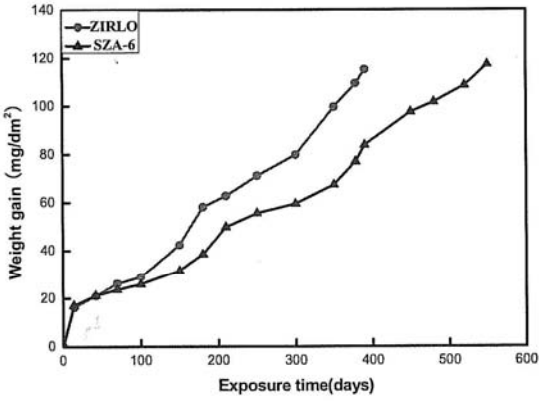

Figure 1. Corrosion weight gain as a function of autoclave test exposure time for button specimens in deionized water at 360℃/18.6MPa. After 390 days exposure, the weight gain of ZIRLO and SZA-6 are 115mg/dm² and 83mg/dm² respectively.

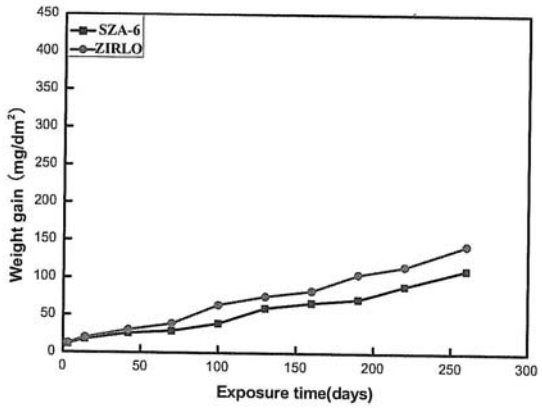

Figure 2. Corrosion weight gain as a function of autoclave test exposure time for button specimens in lithiaed water with 0.01M LiOH at 360℃/18.6MPa. After 260 days exposure, the weight gain of ZIRLO and SZA-6 are 143mg/dm^2 and 110mg/dm^2 respectively.

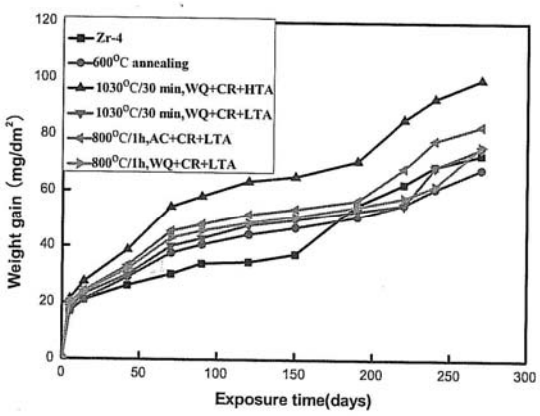

Figure 3. Corrosion weight gain as a function of autoclave test exposure time for small ingot specimens in deionized water at 360℃/18.6MPa. After 270 days exposure, the weight gain of ZIRLO and SZA-6 with 600℃ anneal are 108mg/dm^2 and 68mg/dm^2 respectively.

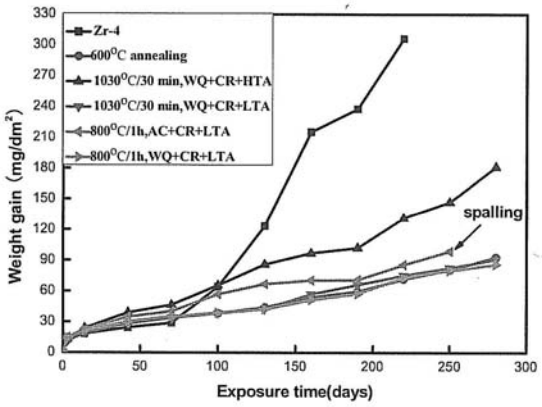

Figure 4. Corrosion weight gain as a function of autoclave test exposure time for small ingot specimens in lithiaed water with 0.01M LiOH at 360℃/18.6MPa. After 280 days exposure, the weight gain of ZIRLO and SZA-6 with 600℃ anneal are 185mg/dm^2 and 93mg/dm^2 respectively.

Effect of Mo on Microstructure and Mechanical Properties in Zr-based Alloys

H. L Yang1, H. Abe2,*, Y. Satoh2, Y. Matsukawa2, T. Matsunaga2

1School of Engineering, Tohoku University, Sendai, 980-8577, Japan
2Institute for Materials Research, Tohoku University, Sendai, 980-8577, Japan

Abstract

In order to meet the ever-increasing demands on the performance of Zr-based alloys for the nuclear reactor core applications, due to advanced design requirement, such as high burnup, long-term operation without incident and troubles, the effects of Mo content on microstructure and mechanical properties of Zr-Nb alloys were systematically studied in this work. The results of XRD analysis indicated that experimental alloys had a typical texture structure after recrystallization caused by cold rolling, and Mo could relax the normal basal texture. The measurement of grain size was carried out by electron back-scattered diffraction (EBSD) analysis, the results suggested Mo could help to refine grain size from 7.8 μm to 2.5 μm. Another profound effect by Mo addition was retardation of recrystallization, which was proved by the results of scanning electron microscope (SEM), which was explained in terms of solute dragging effect of Mo. The BCC structure β-(Nb, Zr) precipitates were identified in Mo-free alloy, and β-(Nb, Mo, Zr) in Mo-contained alloys, by FEI TITAN 80-300 TEM equipped with EDS, which indicated that only trace amounts of Mo was dissolved in Zr-matrix, most of Mo participated in the formation of precipitates. It was clear that the average diameter of precipitates decreased and number density of precipitates improved with the increasing of Mo content according to the measurement by a JEOL JEM-2100 TEM. Mechanical properties, such as hardness, yield strength and ultimate strength, were measured by Vickers hardness and conventional tensile test at room temperature, the mechanical strength is generally interpreted by solid solution hardening, grain refinement strengthening and precipitation hardening, it was found that the grain refinement was the greatest contributor among them in this system. All of these above results indicate that Mo-containing Zr-based alloys are worth investigating as an expected material for the future nuclear power plant.

Effect of Predeformation on Growth Behavior of Second Phase Particles in a Zr-Sn-Nb Alloy During 600-700 °C Aging After β Quenching

Linjiang Chai, Baifeng Luan*, Risheng Qiu, Qing Liu

College of Materials Science and Engineering, Chongqing University, Chongqing, 400044, P. R. China

It is well known that the mechanical properties and corrosion resistance of Zr alloys are sensitive to their microstructures, especially structures, compositions and size distribution of the second phase particles (SPPs). Previously, a number of studies were conducted on the structure identification and the composition measurement of the SPPs in various Zr alloys. However, in spite of its equivalent significance, much less attention has been paid to growth kinetics of these SPPs [1]. This impedes the establishment of clear relationships between SPP sizes in Zr alloys and heat treatment parameters (especially annealing temperature and time). In this work, a Zr-0.85Sn-0.4Nb-0.4Fe-0.1Cr-0.05Cu (in wt.%) is selected to investigate the growth kinetics of the SPPs during 600-700°C aging after β quenching and a 20% predeformation. Attentions are also paid to the evolution of SPPs distribution as the aging proceeds. The as-received Zr sheet (starting materials), supplied by Northwest Institute for Non-ferrous Metal Research (NINMR) of China, were fully recrystallized. Specimens with dimension of 8×6×1.4 mm^3 were cut from the Zr sheet and then β-solution treated at 1030 °C for 40 min and water quenched. The as-quenched specimens were divided into two groups. For the first group, aging at 600-700°C for 30-1800 min was conducted immediately following the β-quenching treatment. For the second group, however, a 20% pre-deformation was performed by a DSI Gleeble 1500D thermomechanical simulator prior to subsequent aging treatments. Microstructures of specimens in both groups were characterized using a transmission electron microscope (ZEISS Libra 200) and a field emission gun scanning electron microscope (FEI Nova 400). For both groups, microstructural observations reveal that the SPPs distribute linearly along the boundaries of α plates at the initial aging stage. As the aging time prolongs and/or temperature increases, the linear distribution feature of SPPs weakens gradually and finally a random distribution is formed. Note that the introduced predeformation is able to promote the transition from linear to random distribution of the SPPs. A numerical analysis confirms that the growth of SPPs in both groups well follows the second order kinetics of Kahlweit theory [2]. The activation energy of SPPs growth is experimentally determined to be 194 kJ/mol in directly aged specimens. However, the introduction of the 20% predeformation decreases the activation energy to 189 kJ/mol.

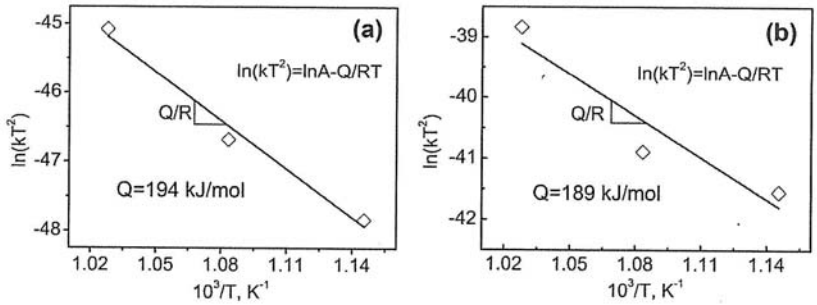

Figure 1. Effect of 20% predeformation on growth activation energy of SPPs in Zr-1Sn-0.4Nb-0.4Fe-0.1Cr-0.05Cu alloy

References

[1] Gros, J. P. Wadier J.F., Precipitate growth kinetics in Zircaloy-4, Journal of Nuclear Materials, 172 (1990) 85-96.

[2] Kahlweit M., Ostwald ripening of precipitates, Advances in Colloid and Interface Science, 5 (1975) 1-35.

THE EFFECT OF TEMPERATURE AND COOLING RATES ON HYDRIDE REORIENTATION OF HIGH BURNUP CLADDINGS UNDER INTERIM DRY CONDITIONS

Su-Jung Min , Myeong-Su Kim , Chu-Chin Won , Kyu-Tea Kim

Dongguk University, College of Energy & Environment, Gyeongju, Gyeongbuk, Republic of Korea

Corresponding author: maymsj1118@dongguk.ac.kr

In this work, the integrity of high burnup spent fuel during the interim dry storage was investigated, simulating interim dry storage and high burnup fuel conditions and using unirradiated Zr-Nb alloy tubes. Cooling-induced hydride reorientation tests were performed from 400°C to the respective temperatures of 300 °C, 200°C and RT at cooling rates of 2 and 7°C/min and then tensile tests were performed for the hydride reoriented specimens. The cooldown test results indicate that the slower cooling rate generated the more radial hydrides and subsequently the severer mechanical performance degradations. In addition, the 250ppm-H specimens generated relatively longer radial hydride plates reprecipitated during the cooldown processes at various cooling rates from the dissolved hydrogen atom in the matrix at 400°C, whereas the 250ppm-H specimens relatively shorter radial hydride plates, which may be caused by some blocking effects of abundant undissolved circumferential hydride plates at 400°C in the latter specimen.

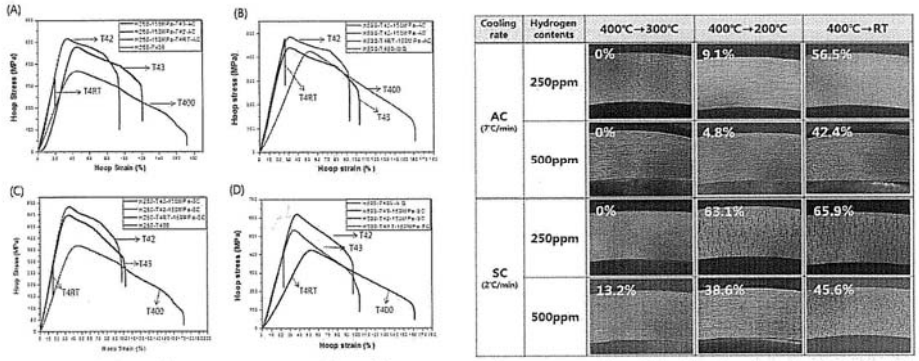

Figure 1. Terminal cooldown-temperature-dependent stress-strain curves and hydride distributions; (a) H250-AC , (b) H500-AC, (c) H250-SC, (d) H500-SC.

[1] B. Choi, Development of Evaluation Technology for Spent Nuclear Fuel Integrity during Interim Dry Storage, 2008, p. 48
[2] USNRC, Cladding Considerations for the Transportation and Storage of Spent Fuel, SFST-ISG-11 Revision 3, 2003
[3] K. Kese, Hydride Re-Orientation in Zircaloy and its Effect on the Tensile Properties, SKI Report, 1998
[4] S. I. Hong, K.W. Lee, J. Nucl. Mater.2005, 340, p203-208
[5] H.C. Chu, S.K. Wu, K.F. Chien, R.C. Kuo, J. Nucl. Mater..2007, 362, p 93-103
[6] J. H. Hong, Nuclear Materials, Hans house , 2012, p 392

Study on direct zirconium powder production by bubble injection of $ZrCl_4$

Hyun-Na Bae[1], Seon-Hyo Kim[1], Go-Gi Lee[2], Mi-Seon Choi[2]
[1]*Department of Materials Science and Engineering, Pohang University of Science and Technology, San31, Hyoja-dong, Nam-gu, Pohang, Gyeongbuk 790-784, Korea*
[2]*Advanced Metallic Materials Research Department, Research Institute of Industrial Science and Technology, San32, Hyoja-dong, Nam-gu, Pohang, Gyeongbuk 790-330, Korea*

The most prevalent method of producing zirconium is Kroll process[1]. But Kroll process has low efficiency due to batch-type process. For this reason, Kroll process needs to decrease processing time and increase productivity. Reduction process using ZrCl4 bubble explored by this research directly could produce metal powder without the existing process of transferring metal sponge into powder. A gaseous form of sublimated ZrCl4 was injected into molten MgCl2 in the form of layer separation between Mg. A bubble form of ZrCl4 rises up, leading a reduction reaction with Mg at the interface between Mg and MgCl2 which eventually caused the production of zirconium which could be found on the bottom of the crucible because specific gravity of zirconium is greater than molten salts. In this research, reduction process using bubble of ZrCl4 was explored experimentally and zirconium powder was produced actually. Obtained zirconium powder which was eliminated impurities including remained molten salts was investigated in terms of morphology and chemical analysis shown in Figure 1 and 2. Thus, this study is meaningful as it gives feasibility of continuous production of Zr powder.

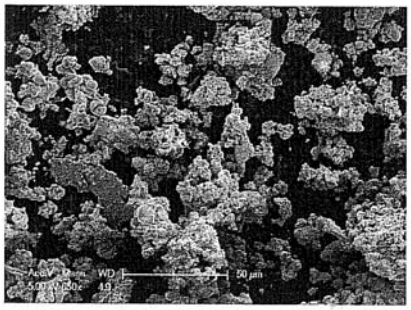

Figure 1. SEM imege of Zr powder

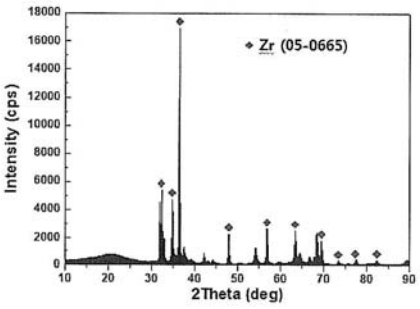

Figure 2. XRD pattern of Zr powder

References

[1] F. G. Reshetnikov, E. N. Oblomeev, Mechanism of formation of zirconium sponge in zirconium production by the magnesothermic process, The Soviet Journal of Atomic Energy, 1957, 561-564

Effect of Sn content on the phase transformation of Zr-Sn-Nb-Fe alloys

Cheng Zhuqing*, Yang Zhongbo, Zhao Wenjin, Yi Wei

Reactor Fuel and Material Key Laboratory, Nuclear Power Institute of China,
Chengdu, China, 610041
*Corresponding author, phone:+86-28-85906033, email: czhq07@163.com

Abstract

Sn is one of the main alloying elements in zirconium alloys, its content in alloy could change the transformation temperature from α to β phase, and also has a significant effect on the manufacturing process and performance of alloy. In the present work, the effect of Sn content on the phase transformation temperature of Zr-x wt%Sn-1 wt%Nb-0.3 wt%Fe (x=0, 0.4, 0.8, 1.0, 1.2, 1.5) alloys was systematically studied by DSC and metallographic technology. Due to the accuracy limitation of calorimetric measurements, the α/α+β and α+β/β phase transformation temperatures are over- and under-estimated, respectively. The results showed that the α/α+β phase transformation temperature for Zr-Sn-Nb-Fe alloys increased with the increase of Sn content, which conforms that Sn is an element of extending the α region. Besides, the alloys specimens were heated at the given phase transformation temperature obtained by DSC and quenched in water, and then observed by OM and SEM to know more information about the relation between β phase formation and heat temperature. It was showed that the temperature was lower and more accurate than that obtained by DSC.

Key words: Zirconium alloys; Phase transformation temperature; DSC

Effect of Pre-hydriding on the Burst Behavior of the Zirconium Cladding under Loss-of-Coolant Accident Condition

Dong Jun Park[a], Jeong Yong Park[a], Hyun Gil Kim[a], Yang Il Jung[a], Jong Sung Yoo[b], Mok Yong Kyoon[b], and Jung Min Suh[b]

[a]*Korea Atomic Energy Research Institute, 989-111 Daedeok-daero, Yuseong-gu, Daejeon, 305-353, Republic of Korea*

[b]*KEPCO Nuclear Fuel, 989-242, Daedeok-daero, Yuseong-gu, Daejeon, 305-353, Republic of Korea*

To investigate effects of hydrogen on the rupture behavior and mechanical property of ballooned zirconium cladding after loss-of-coolant accident, simulated loss-of-coolant accident tests were carried out using the pressurized zirconium tube samples with and without hydrogen pre-charging. Pre-hydrided cladding sample showed a lower deformation in ballooned area and lower rupture temperature than as-received cladding sample. Ballooned cladding without hydrogen charging showed no significant difference in mechanical property in spite of a wide range of values for circumferential strain and different balloon shape caused by different heating rate. Pre-hydrided cladding, however, showed an increase in maximum load with increasing heating rate. Strong relationship between hydrogen content and burst behavior during loss-of-coolant accident was analyzed and the mechanism of hardening by hydrogen in zirconium alloy was explained.

Study on Hydride Reorientation of Cladding Tubes Simulating Spent Nuclear Fuel under Interim Dry Storage

Ju-Jin Won*, Su-Jung Min, Myeong-Su Kim, Kyu-Tea Kim
Nuclear and Energy Engineering Department, Dongguk University
123, Dongdea-Ro, Gyeongju, Republic Of Korea, 780-714
Corresponding author: chuchinwon@dongguk.ac.kr

The spent nuclear fuel rods with different oxide thicknesses and hydrogen contents under interim dry storage may experience various peak temperatures, persistent cooldown with various cooling rates and tensile hoop stresses on the cladding. For the evaluation of the effects of aforementioned various dry storage conditions on the spent nuclear fuel rods, therefore, two kinds of peak temperatures of 300 and 400°C, three kinds of cooling rates of 2, 4 and 15 °C/min from the two respective peak temperatures and three kinds of tensile hoop stress of 80, 100 and 150MPa were employed for the 300ppm hydrogen charged Zr-Nb cladding ring specimens with about 5um oxide. After the cooldown tests, microstructure examinations were performed to analyze hydride distributions in the cladding ring specimens and then tensile tests were carried out to analyze mechanical property degradations and hydride-induced brittle behaviors. The cooldown test results indicate that the slower cooling rate and the higher peak temperature generated the larger radial hydride reorientation and the longer hydride. The tensile test results show that the slower cooling rate generated the larger decrease in cladding elongation and the higher peak temperature caused the larger decrease in cladding ultimate tensile strength and elongation. In addition, the slower cooling rate generated the more cleavage fracture surfaces. These hydride reorientation-dependent phenomena may be explained by the hydrogen dissolution at the peak temperatures, the hydrogen precipitation during the cooldown processes, and the extent of hydride reorientation and morphology.

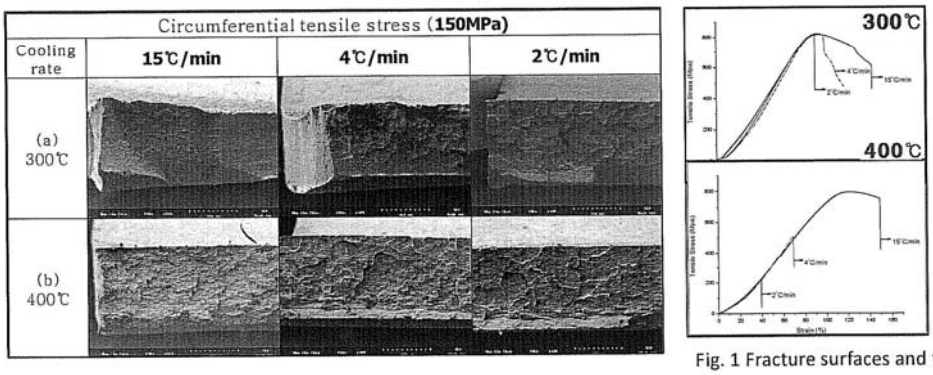

Fig. 1 Fracture surfaces and tensile stress-strain curves for 300ppm-H Zr-Nb cladding ring specimens.

REFERENCES

[1] Y.S. Kim et all, "Development of Spent Fuel Integrity Evaluation Technology for the Long-term Dry Storage". KAERI/CM-1397(2010)
[2] H. Kim, Y. Jeong, K. Kim, Nucl.Eng.Tech.49,249(2010)

[3] J. P. Mardon, A. Lesbros, C. Bernaudat, and N. Waeckel, Proc. of the 2004 Int. Meeting on LWR Fuel Performance, p. 507, Orland, FL (2004).
[4] K. Kllstrm, Scandinavian Journal of Metallurgy 4, p, 65(1975).

HIGH TEMPERATUR STABILITY OF DELTA-PHASE ZIRCONIUM HYDRIDE

Ken Kurosaki, Daichi Araki, Hiroaki Kimura, Yuji Ohishi, Hiroaki Muta, and Shinsuke Yamanaka

Division of Sustainable Energy and Environmental Engineering, Graduate School of Engineering, Osaka University, 2-1 Yamadaoka, Suita-Shi, Osaka 565-0871, Japan

Our group has investigated the physical and chemical properties of Zr hydrides with various hydrogen contents [1]. Here, polycrystalline bulk samples of δ-phase Zr hydride ($ZrH_{1.6}$) were prepared and their high-temperature stability was investigated. The phase structure was examined between room temperature and 973 K using high-temperature X-ray diffraction (XRD) and thermogravimetric-differential thermal analysis (TG-DTA). The results of high-temperature XRD and TG-DTA measurements carried out in both helium/argon and air indicated that at high temperatures, the release of hydrogen is accompanied by a reduction in the intensity of peak associated with the δ-phase Zr hydride. In addition, peaks due to ZrO_2 and apparently ε-phase Zr hydride appear only for the measurements carried out in air. It is considered that both hydrogen release and oxidation occur as the temperature increases.

[1] S. Yamanaka et al., Characteristics of zirconium hydride and deuteride, *J. Alloys Compd.* **330-332**, 99-104 (2002).

Mechanical Properties at High Temp.

Bulk Hydride is brittle ? until ? Temp.

A Study on the Effects of Dissolved Hydrogen on Zirconium Alloys Corrosion

Yong-soo Kim [a], Yong-hwan Jeong[b], and Seung-beom Son [c]*
[a]Hanyang University, Seoul 133-791, Korea*
[b]Korea Atomic Energy Research Institute, Daejeon 305-353, Korea
[c]Korea Nuclear Fuel Co., Ltd., Daejeon 305-353, Korea
[*]Corresponding author: Tel:+82-2-2220-0467, Fax:+82-2-2281-5131,
Email: yongskim@hanyang.ac.kr

Abstract

The effects of dissolved hydrogen on oxide phase transformation and micro-structural changes during zirconium oxide growth were investigated using Raman spectroscopy and Transmission Electron Microscopy (TEM).

Raman spectra measurements show that tetragonal zirconia develops during oxide growth and a fraction of the phase in pre-hydrided alloy is consistently lower than that of an un-hydrided one. This was observed identically in both Zircaloy-4 and Zr-1.5Nb alloys.

TEM analysis at the metal-oxide interface support that the Raman spectra changes resulted from micro-structural changes.

These results suggest that the dissolved hydrogen may cause meta-stabilization of the tetragonal phase oxide grown at the metal-oxide interface, probably by relaxing the compressive stress built up at the interface, or by modifying the stress distribution over the interface. The relaxation or modification possibly comes from the mitigation of the lattice incoherency between the metal and the oxide at the interface that is the origin of the compressive stress build-up.

Hydrogen Effect of Zircaloy-4 on the High Pressure Steam Oxidation.

Yunmock Jung[1] , Kwangheon Park[1*] , Seonggi Jeong[1]

[1]*Department of Nuclear Engineering, Kyunghee University, Kyunggi-do, 446-701*
[*]*Corresponding author: kpark@khu.ac.kr*

ABSTRACT

The characteristics of oxidation for the Zry-4 was measured in the 800℃ and high steam pressure(50bar, 75bar, 100bar) conditions, using an apparatus for high pressure steam oxidation. The effect of accelerated oxidation by high-pressure steam was increased more than 60% in hydrogen-charged cladding than normal cladding. This difference between these oxidation amount tends to be larger as the higher pressure. The accelerated oxidation effect of hydrogen charging cladding is regarded as the hydrogen on the metal layer affects the formation of the protective oxide layer. The creation of the sound monoclinic phase in Zry-4 oxidation influences reinforcement of corrosion-resistance of the oxide layer. The oxidation is estimated to be accelerated due to the creation of equiaxial type oxide film with lower corrosion resistance than that of columnar type oxide film. When tetragonal oxide film transformed into the monoclinic oxide film, surface energy of the new monoclinic phase reduced by hydrogen in the metal layer.

Experimental

1. Specimen

Table 1. Chemical composition of specimen.

(wt%)	Zr	Nb	Sn	Fe	Cr
Zry-4	bal.	-	1.35	0.2	0.1

2 Apparatus

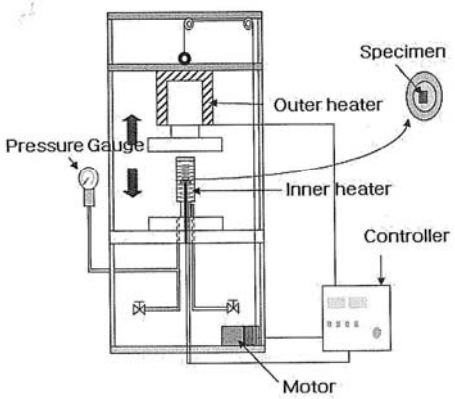

Figure 1. Experiment apparatus

Results

Figure 2 shows the result of the weight gain of Zry-4 specimens containing 800ppm of hydrogen and those of normal (hydrogen free) Zry-4 specimens at 800℃. High pressure steam enhanced the oxidation of both normal and hydrogen-containing specimens. The enhancement of oxidation by high-pressure steam was more severe to the specimen containing hydrogen.

At 800C, the hydrogen of 800ppm fully dissolves into Zry-4 cladding matrix. Hence, the increased enhancement was due to the hydrogen dissolved.

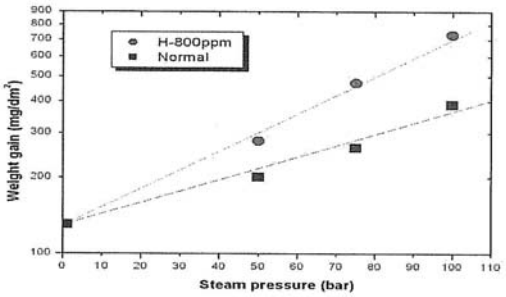

Figure 2. Experimental results of the weight gain of specimens at 800℃ in some steam pressure for 1500sec.

The microstructures of the H-dissolved Zry-4 specimens after the oxidation test are shown in figure 3. The oxide layer was not uniform if the specimen was oxidized at high pressure steam. As steam pressure increased, the oxide contained large vertical (to the surface) cracks.

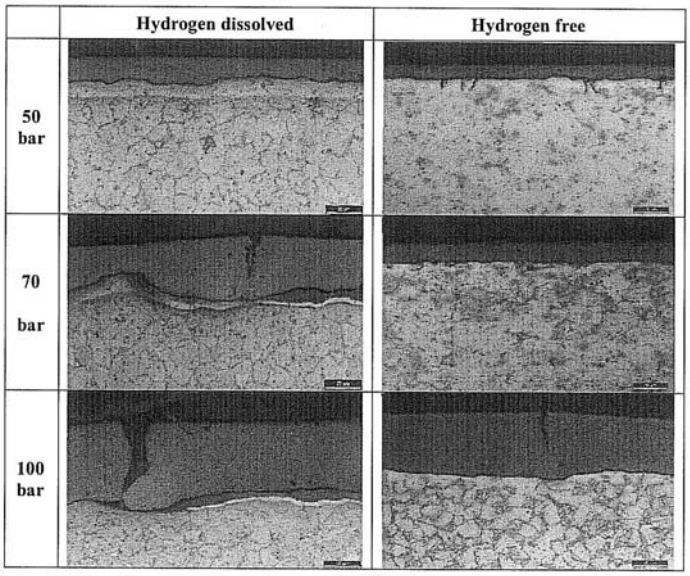

Figure 3. Microstructures of specimens at 800℃ in some steam pressure for 1500sec.

REFERENCES

[1] K. Park, S. Yang, and K. Ho, The Effect of High Pressure Steam on the Oxidation of Low-Sn Zircaloy-4, Journal of Nuclear Materials, vol. 420, p.39, 2012

[2] K. Park, K. Kim, T. Yoo, and K. Kim, Pressure Effect on High Temperature Steam Oxidation of Zircaloy-4, Metals and Materials International, vol. 7, p.367, 2001

[3] B. Cox, Accelerated Oxidation of Zircaloy-2 in Supercritical Steam, AECL-4448, 1973

[4] R. E. Pawel, J. V. Cathcart, and J. J. Campbell, The Oxidation of Zircaloy-4 at 900 and 1100 in High Pressure Steam, Journal of Nuclear Materials, vol. 82, p. 129, 1979

Influence of Second-phase Particles on Hydrogen Absorption and Desorption Behavior of N36 Cladding

Chen Liang*, Yang Zhongbo, Liu Lili, Sun Chao

(Science and Technology on Reactor Fuel and Materials Laboratory, Chengdu)

* Corresponding author, Tel: 0086-28-85903294, E-mail: winforce1982@126.com

Abstract

The hydrogen absorption and desorption behavior of N36 zirconium alloy cladding tubes with the different second phase particles (SPPs) were investigated by the dry-type hydrogenation and thermogravimetry tests. The SPPs in N36 finished product cladding were characterized by scanning electronic microscope (SEM) and the size distribution of SPPs was statistically calculated. The results showed that the N36 specimens with the coarse SPPs excelled the specimens with a fine and evenly distributed SPPs in hydrogen absorption and desorption abilities. The N36 specimens with coarse SPPs absorbed and desorbed hydrogen easily with higher speed. The reason was that such heat treatment could make to increase the size of SPPs in α-Zr matrix. However the heat treatments had a less influence on hydrogen absorption and desorption of N36 than that of Zr-4. This may be the reason that the $Zr(Nb, Fe)_2$ SPPs in N36 alloy is less reactive with hydrogen than that of $Zr (Fe, Cr)_2$ SPPs in Zr-4. The amount of hydrogen absorption and desorption was closely related to the SPPs size and category. These $Zr(Nb, Fe)_2$ SPPs with higher reversible absorbing and desorbing ability than α-Zr matrix played a role as a preferred path for hydrogen uptake.

Key words: hydrogen absorption; second phase particles (SPPs); zirconium alloy

EFFECT OF HYDROGEN ON THE OXIDATION KINETICS OF ZIRCALOY-4 CLADDING AT 650℃ IN AIR

Jen-Hung Chen *, Wen-Chen Liao
Institute of Nuclear Energy Research, Taiwan
* Corresponding author: jhchen@iner.gov.tw

The kinetics of Zircaloy fuel cladding oxidation in air is an important subject for many safety-related studies. Major examples are the fuel cladding oxidation under the loss of water accident of spent fuel storage pool and the reactor pressure vessel breaching following a thermal shock event. Another example is the spent fuel rods interaction with the intrusive air under the structural failure of dry storage and transportation cask. The objective of this study is to obtain experimental data on the air oxidation kinetics of un-irradiated Zircaloy-4 cladding with hydrogen contents of 100 ppm ~ 1000 ppm that is representative of the current inventory of spent fuel discharged under various levels of fuel burnup. The oxidation tests were conducted at 650℃ at which the hydrided Zircaloy-4 cladding specimens were oxidized with hydrogen in a state of solid solution.

Thermogravimetric analyser (TGA) with accuracy of 0.1μg was used for the continuous monitoring of weight gain during oxidation. Zircaloy-4 cladding tube segments with a dimension of 10 mm long, outer diameter 9.5 mm and inner diameter 8.4 mm, under various conditions of as-received, 120 ppm, 350 ppm and 750 ppm hydrided, were tested at 650℃ in air for 50 hours exposure. The results indicate that the hydrided specimens revealed a higher oxidation kinetics and approximately obeyed a parabolic rate law before the transition. After transition, however, all the specimens obeyed a linear rate law and had the similar rate constants, as shown in Fig. 1. The zirconium hydrides dissolved in Zircaloy-4 matrix during 650℃ exposure and precipitated at grain boundary after cooling to room temperature, as demonstrated in Fig.2. It is concluded that hydrogen in a solution state in Zircaloy-4 increases the initial parabolic oxidation kinetics and results in a later kinetic transition to linear regime.

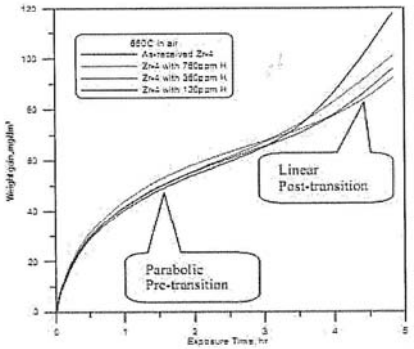

Figure 1. Weight gain against exposure time in 650℃ air for the hydrided Zircaloy-4 tube specimens.

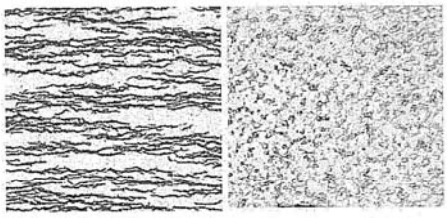

(a) before oxidation (b) after oxidation

Figure 2. Hydride morphology: (a) before oxidation showing the circumferential hydrides, (b) after oxidation showing hydrides precipitated at grain boundary.

Curve-fitting on the Thermophysical properties of N36 alloy

Wu Songling*, Dai Xun, Yang Xiaoxue
Reactor Fuel and Material Key Laboratory, Nuclear Power Institute of China,
Chengdu, China, 610041
*Corresponding author, phone:+86-28-85903969, email: slwucn@163.com

Abstract

Thermophysical properties of zirconium alloys include thermal conductivity, specific heat capacity, thermal expansion, elastic modulus and Poisson's ratio, which are difficult to be measured at high temperature and high vacuum condition. This paper describes a method to get the thermophysical properties of N36 alloy, which is curve fitting based on thermophysical properties results of other zirconium alloys (ZIRLO,M5,Zr-4). The fitting results show that the thermal conductivity of N36 alloy is given by λ=10.478+0.0137*T when T is below 1200℃.The specific heat capacity is given by Cp=0.24367+1.53E-4* T when T is bellow 700℃ and Cp=-17.714+0.04185 T-2.38E-5 T2 while T is at the range of 700℃ to 1000℃,when the temperature is up to 1000℃,the specific heat capacity is nearly a constant of 0.3561 J/g•K. The axial and radial coefficients of thermal expansion are different because of anisotropy. The former is given by =-0.01103+5.2607E-4*T when T is below 800℃ or up to 1000℃,at the range of 800℃ to 1000℃, the value is nearly a constant of 0.439, The latter is given by =A+B*T, where A=-0.0122 and B=5.8E-4 when T is less than 800℃ or more than 1000℃,whereas A=-0.0136, B=5.82E-4 when 800 ℃<T<1000℃. The elastic modulus is linear with temperature and given by E=111.3-0.0693*T, where T is below 1200℃;the Poisson's ratio is pretty sensitive to the component of the zirconium alloy, which is need further test to quantify the value. The fitting data of N36 alloy are close to the results tested when the temperature is bellow 800℃, and it makes sense to forecast the thermophysical properties of N36 alloy at high temperature according to the fitting curves.

Key words: N36 zirconium alloys; Curve-fitting; Thermophysical properties

SOME INVESTIGATIONS IN THE ZIRCALOY PICKLE SALTS

H.F. Gu[a,b], L. F. Zhang[a,b], S.Q. Wu[a,b], G.P.Li[a,*]

[a]*Institute of Metal Research, Chinese Academic of Sciences, 72 Wenhua Road, Shenyang 110016, China*

[b]*University of Chinese Academy of Sciences, Beijing 100039, China*

[c] *State Nuclear Bao Ti Zirconium Industry Company, Baoji 721000, China*

**Corresponding author: gpli@imr.ac.cn*

ABSTRACT

The pickling of Zircaloy with HF-HNO_3solution is a standard and economical practice in the nuclear materials industry. However, the possibility of retaining residual etchant fluoride affects further reactor application of Zircaloy. In order to fully understand Zircaloy pickle bath salts, the compounds obtained by dropping xHF(40 wt.%)-(1-x)HNO_3(65~68 wt.%) solution (where $80 \leq x \leq 100$ Vol.%) on the surface of Zircaloy 4samples at room temperature were investigated. Among these compounds, $ZrF_4(H_2O)$ and $ZrF_4(HF)(3H_2O)$ crystals were both identified by using X-ray diffraction (XRD). When HNO_3 was included in the acid solution used, NH_4ZrF_5 was also identified by employing X-ray diffraction (XRD), X-ray Photoelectron Spectroscopy (XPS) and Infrared Spectroscopy. It was noticed that with the concentration of HF decreasing and that of HNO_3increasing, that is, with x decreasing (where $80 \leq x \leq 100$ Vol.%), the weight fraction of $ZrF_4(HF)(3H_2O)$ decreased while that of NH_4ZrF_5 increased.

Key words:
Zircaloy, HF+HNO_3 solution，$ZrF_4(HF)(3H_2O)$ ，NH_4ZrF_5

Effect of Anneal Temperature on the Hydrogen Orientation of SZA-1 and SZA-3 Alloys

Sheng Peng[1]*, Tian G. Zhang[1], Lian Wang[1], Gai H. Yuan[1] and Xiao S. Li [1],Liutao Chen[2], Jun Tan[2], Hong Zou[2],Rui Li[2], Dungu Wen[2]

1. SNZ, Baoji, Shaanxi 721013, P. R. China

2. China Nuclear Power Technology Research Institute, Shenzhen of Guangdong Prov.518026,China

Corresponding author: pengsheng@sn-zr.com

Hydrogen orientation factor（Fn） is a very important performance index for zirconium alloy cladding tube. According to the ASTM B353, Stress relief annealed specimens shall have an Fn value not more than0.30.Recrystallization annealed specimens shall have an Fn value not greater than0.50. Firstly, the relationship between vicker hardness and anneal temperature of SZA-1 and SZA-3 alloys was obtained。Via the vicker hardness curve , 470℃ was choosed as Stress Relieving Anneal (SRA) and 560℃ as Recrystallization Anneal （RXA） temperture .Hydrogen was introduced into Cold work (CW) , Stress Relieving Anneal (SRA) and Recrystallization Anneal （RXA） sample by hydrogen gas. The result shows that the Fn of CW sample and SRA sample is lower than 0.1. The Fn of RXA sample is around 0.2.Generally , it can be summarized that hydrogen orientation mainly depends on the radial texture factor (fr). Based on the test date, there is little differences among these samples. We can conclude that the hydrogen orientation of CW sample, SRA sample and RAX sample is related to the anneal temperature. The circumferential residual compressive stress exists in the tube when the anneal temperature is 470℃. The hydride distributes along the circumferential direction. On the contrary, when the anneal temperature is 560℃, the tubes has less circumferential residual compressive stress. The hydrogen orientation mainly depends on the fr.

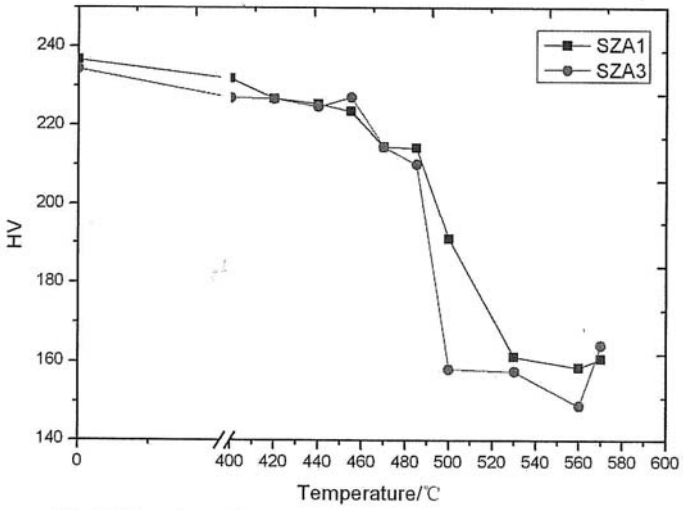

Fig.1 Effect of anneal temperature on HV of SZA1 and SZA3 Tubes

Table 1 fr of SZA1 and SZA3 tubes

	CW	SRA	RAX
SZA1	0.57	0.50	0.56
SZA3	0.55	0.50	0.54

List of Participants

Organizing Committee

Bangxin Zhou	**Shanghai University** P.O.Box 269,Institute of Materials,149Yanchang Road, Shanghai, 200072, P.R. China zhoubx@shu.edu.cn
Gaihuan Yuan	**State Nuclear Baoti Zirconium Industry Company** No.206,High Tech Road SNZ, Baoji,Shaanxi, 721013,P.R. China ygh@sn-zr.com
Qing Liu	**Chongqing University** Room 519, Comprehensive Experiment Building, Campus A of Chongqing University,Chongqing,400044,P.R. China qingliu@cqu.edu.cn
Wenjin Zhao	**Nuclear Power Institute of China** 核动力研究院 No.28 3rd Section of South 1st Ring Road, Chengdu,610041,P.R. China zhaowj@npic.ac.cn
Zhongkui Li	**Northwest Institute For Non-ferrous Metal Research** No.96,Weiyang Road, 710016,Xi'an,Shaanxi, China lizhangyi@c-nin.com

Advisory Committee

Kyu Tae Kim	**Dongguk University** 707 Sekjang-dong,Gyengju,Gyeongsangbuk-do,708-714,South Korea ktkim@dongguk.ac.kr
Roang-Ching Kuo	**Institute of Nuclear Energy Research** No.1000,Wenhua Rd, Jiaan Village,Longtan Township,Taoyuan County,32546,Taiwain rckuo@iner.gov.tw
Sadaaki Abeta	**Mitsubishi Nuclear Fuel** Mitsubishi Nuclear Fuel Co.,Ltd.,12-1,Yurakucho I-Chome, Chiyoda-ku,Tokyo, 100-0006,Japan Saddki.abeta@mitsubishicorp.com

Sakamoto Kan	**Nippon Nuclear Fuel Development Co.Ltd(NFD)** 2163,Narita-Cho, Oarai-Machi.Higashi Ibaraki-Gun,Ibaraki-Ken 311-1313 JAPAN Kan.Sakamoto@nfd.co.jp
Shinsuke Yamanaka	**Osaka University** 2-1 Ymadaoka,Suita Osaka,565-0871,Japan yamanaka@see.eng.osaka-u.ac.jp
Yong Hwan Jeong	**Korea Atomic Energy Research Institute** 989-111 Daedeok-daero,Yuseong-gu,Daejeon,305-353,South Korea yhjeong@kaeri.re.kr

Registered Participants

Baifeng Luan	**Chongqing University** Room 509, Comprehensive Experiment Building, Campus A of Chongqing University, Chongqing,400044,P. R. China bfluan@cqu.edu.cn
Chan Hyun Park	**KEPCO Nuclear Fuel** Kepco NF TSA Plant,8,Techno 6-ro, Yuseong-gu,Daejeon, Korea Rep. chpark@knfc.co.kr
Dong Jun Park	**Korea Atomic Energy Research Institute** 989-111 Daedeok-daero, Yuseong-gu, Daejeon, 305-353, South Korea pdj@kaeri.re.kr
Donghui Kim	**KEPCO Nuclear Fuel TSA** 688 KNFCTSA Gwanpyeong-dong,Yuseong-gu,Daejeon, Korea Rep. donghui@knfc.co.kr
Dungu Wen	**China Nuclear Power Technology Research Institute Co., Ltd** 1218 Block A, Jiangsu Building, Yitian Road, Futian District, Shenzhen, P. R. China wendungu@cgnpc.com.cn

Gang Li	**State Nuclear Baoti Zirconium Industry Company** No.206,High Tech Road SNZ, Baoji,Shaanxi, 721013,P.R. China llkkjj11@163.com
Geping Li	**Institute of Metal Research, Chinese Academic of Sciences** 72 Wenhua Road, Shenyang, China gpli@imr.ac.cn
Han Ok Ryu	**KEPCO Nuclear Fuel** Kepco NF TSA Plant,8,Techno 6-ro, Yuseong-gu,Daejeon, Korea Rep. horyu@knfc.co.kr
Hengfei Gu	**Institute of Metal Research, Chinese Academic of Sciences** 72 Wenhua Road, Shenyang, China hfgu12s@imr.ac.cn
Hong Guo	**China North Nuclear Fuel Co.Ltd** No.456 Qingshan District, Baotou, China ke_ji_chu@163.com
Hui Li	**Chungnam National University** 99 Daehak-ro,Yuseong-gu,Dasjeon 305-764 KOREA
Huilong Yang	**Tohoku University** 2-1-1 Katahira, Aoba-ku, Sendai 980-8577,Janpan yanghuilong@imr.tohoku.ac.jp
Hyun-Gil Kim	**Korea Atomic Energy Research Institute** 989-111 Daedeok-daero, Yuseong-gu, Daejeon,305-353,South Korea hgkim@kaeri.re.kr
Il-Hyun Kim	**Korea Atomic Energy Research Institute** 989-111 Daedeok-daero, Yuseong-gu, Daejeon,305-353, South Korea s-weat@hanmail.net

In Seon Hwang	**KEPCO Nuclear Fuel** Kepco NF TSA Plant,8,Techno 6-ro, Yuseong-gu,Daejeon, Korea Rep. ishwang@knfc.co.kr
Jen-Hung Chen	**Institute of Nuclear Energy Research** No.1000, Wenhua Rd., Jiaan Village, Longtan Township, Taoyuan County, 32546, TAIWAN jhchen@iner.gov.tw
Jeong Yong Park	**Korea Atomic Energy Research Institute** 989-111, Daedeok-daero, Yuseong, Daejeon 305-353, Republic of Korea parkjy@kaeri.re.kr
Ji Eun Lee	**KEPCO Nuclear Fuel TSA** 688 KNFCTSA Gwanpyeong-dong,Yuseong-gu,Daejeon, Korea Rep. jieun@knfc.co.kr
Jianyun Shen	**General Research Institute for Nonferrous Metals** No.2. Xinjiekouwai Road , Beijing,100088,China grinmshen@hotmail.com
Jing Zhou	**State Nuclear Baoti Zirconium Industry Company** No.206,High Tech Road SNZ, Baoji,Shaanxi, 721013,P.R. China mulle @163.com
Jinlong Zhang	**Shanghai University** P.O.Box 269,Institute of Materials,149 Yanchang Road, Shanghai, 200072,P.R .China jlzhang@shu.edu.cn
Jong Han Moon	**KEPCO Nuclear Fuel TSA** 688 KNFCTSA Gwanpyeong-dong,Yuseong-gu,Daejeon, Korea Rep. jhmoon@kndc.co.kr
Jong Hyeon Lee	**Chungnam National University** 99 Daehak-ro, Yuseong-gu, Daejeon 305-764,KOREA jonglee@cnu.ac.kr

	Jongyeol Kahng	**KEPCO Nuclear Fuel TSA** 688 Gwanpyeong-dong,Yuseong-gu, Daejeon 305-509，Korea Rep. jykahng@knfc.co.kr
	Joon Ro Lee	**KEPCO Nuclear Fuel** KEPCO NF,242,Daedeol-daero 989 beon-gil Yuseong-gu, Daejeon, Korea Rep. jrlee@knfc.co.kr
	Ju Jin Won	**Dongguk University** 707 Seokjang-Dong, Gyeongju, Gyeongbuk, South Korea wjj611@nate.com
✓	Kazuaki Yanagisawa	**Japan Atomic Energy Agency** 1233 Watanuki Takasaki Gunma, JAPAN yamaqisawa.kazuaki@jaea.go.jp
	Ke-qiang Sun	**Nuclear Power Institute of China** No.28 South Third Section Yihuan Road Chengdu P.R.China abcsunke@163.com
	Kibum Park	**KEPCO Nuclear Fuel TSA** 688 Gwanpyeong-dong,Yuseong-gu, Daejeon 305-509，Korea Rep. kibum@knfc.co.kr
✓	KUROSAKI Ken	**Osaka University** 2-1 Yamadaoka, Suita, Osaka 565-0871, Japan kurosaki@see.eng.osaka-u.ac.jp
	KyungTae Kim	**KyungHee University** 1732 Deogyeong-daero, Giheung-gu, Yongin-si, Gyeonggi-do kkt8587@khu.ac.kr
	Le Chen	**Nuclear Power Institute of China** No.28 South Third Section Yihuan Road Chengdu P.R.China jolin0102@126.com

Liang Chen	**Nuclear Power Institute of China** No.28 South Third Section Yihuan Road Chengdu P.R.China windforce1982@126.com
Lifeng Zhang	**Institute of Metal Research, Chinese Academic of Sciences** 72 Wenhua Road, Shenyang, China lfzhang11s@imr.ac.cn
Linhua Chu	**State Nuclear Baoti Zirconium Industry Company** No.206,High Tech Road SNZ, Baoji,Shaanxi, 721013,P.R. China chulinhuascu@163.com
Linjiang Chai	**Chongqing University** Room 510, Comprehensive Experiment Building, Campus A of Chongqing University, P. R. China chailinjiang@yahoo.cn
Liutao Chen	**China Nuclear Power Technology Research Institute Co., Ltd** 1218 Block A, Jiangsu Building, Yitian Road, Futian District, Shenzhen, P. R. China chenliutao@cgnpc.com.cn
Meiyi Yao	**Shanghai University** P.O.Box 269,Institute of Materials,149 Yanchang Road, Shanghai, 200072,P.R .China yaomeiyi@shu.edu.cn
Meng Xie	**Nuclear Power Institute of China** No.28 South Third Section Yihuan Road Chengdu P.R.China 992621250@qq.com
Meng Yan	**Nuclear Power Institute of China** No.28 South Third Section Yihuan Road Chengdu P.R.China yanmeng_spring@163.com
Min Young Choi	**KEPCO Nuclear Fuel** #242, Daedeok-daero 989beon-gil, Yuseong-gu Daejeon, 305-353, South Korea mychoi@knfc.co.kr

NaBae Hyun	**Pohang University of Science and Technology** San31, Hyoja-dong, Nam-gu,Pohang,Gyeongbuk 790-784,Korea arihynna@postech.ac.kr
Pengfei Wang	**Nuclear Power Institute of China** No.28 South Third Section Yihuan Road Chengdu P.R.China wpf03082108@163.com
Qifeng Zeng 曾奇锋	上海核工程研究設計院 **Shanghai Nuclear Engineering Research & Design Institute** No.29 Hongcao Road, Xuhui District, Shanghai zengqifeng@snerdi.com.cn
Rui Li	**China Nuclear Power Technology Research Institute Co., Ltd** 1218 Block A, Jiangsu Building, Yitian Road, Futian District, Shenzhen, P. R. China li-rui@cgnpc.com.cn
Sangjin Han	**KEPCO Nuclear Fuel TSA** 688 Gwanpyeong-dong,Yuseong-gu, Daejeon 305-509，Korea Rep. sjinhan@knfc.co.kr
Seonho Noh	**Kyung Hee University** Department of Nuclear Engineering, Kyung Hee University, Yongin-city,Kyunggi-do,446-701, Korea dark@khu.ac.kr
Seung Hyun Kim	**Chungnam National University** 99 Daehak-ro, Yuseong-gu, Daejeon 305-764,KOREA ilbetheone@cnu.ac.kr
Sheng Peng	**State Nuclear Baoti Zirconium Industry Company** No.206,High Tech Road SNZ, Baoji,Shaanxi, 721013,P.R. China pengsheng@sn-zr.com
Songling Wu	**Nuclear Power Institute of China** No.28 South Third Section Yihuan Road Chengdu P.R.China slwucn@163.com

Su Jung Min	**Dongguk University** 707 Seokjang-Dong, Gyeongju, Gyeongbuk, South Korea maymsj1118@hanmail.net
Tan Jun	**China Nuclear Power Technology Research Institute Co., Ltd** 1218 Block A, Jiangsu Building, Yitian Road, Futian District, Shenzhen, P. R. China juntan_june@aliyun.com
Tianguo Wei	**Nuclear Power Institute of China** No.28 South Third Section Yihuan Road Chengdu P.R.China wtg05@163.com
Weon Mo Kang	**KEPCO Nuclear Fuel** Kepco NF TSA Plant,8,Techno 6-ro, Yuseong-gu,Daejeon, Korea Rep. wmkang@knfc.co.kr
Xinyi Li	**Chongqing University** College of Materials Science and Engineering, Chongqing University, Chongqing 400044, China lixinyide1210@126.com
Xun Dai	**Nuclear Power Institute of China** No.28 South Third Section Yihuan Road Chengdu P.R.China 164714098@qq.com
Yong Kyoon Mok	**KEPCO Nuclear Fuel** 1047 Daedeok-daero, Yuseong-gu, Daejeon,305-353,South Korea ykmok@knfc.co.kr
Yonggang Ren	**China North Nuclear Fuel Co.Ltd** No.456 Qingshan District, Baotou, China ke_ji_chu@163.com
Yong-soo Kim	**Hanyang University** 17 Haengdang-Dong, Sungdong-Gu, Seoul, Korea yongskim@hanyang.ac.kr

Yunhan Ling	**Tsinghua University** Tsinghua Park, Haidian District, Beijing，P.R.China yhling@mail.tsinghua.edu.cn
Yunmock Jung	**KyungHee University** Seocheon-dong, Giheung-gu, Yongin-si Gyeonggi-do 446-701, Republic KOREA
Zhongbo Yang	**Nuclear Power Institute of China** No.28 South Third Section Yihuan Road Chengdu P.R.China yangzhongb@mails.ucas.ac.cn
Zhuqing Cheng	**Nuclear Power Institute of China** No.28 South Third Section Yihuan Road Chengdu P.R.China czhq07@163.com

附錄二 核研所簡報內容

Effect of Hydrogen on the Oxidation Kinetics of Zircaloy-4 Cladding at 650℃ in Air

Presented at
2nd Asian Zirconium Workshop
Baoji, Shaanxi, China
October 15~19, 2013

By
Jen-Hung Chen

Institute of Nuclear Energy Research

Outline

- Introduction
- Experimental
- Results
- Conclusions

Introduction

- A study of spent fuel cladding oxidation in air
  - Under the abnormal loss of coolant of spent fuel storage pool and the structural failure of dry storage
  - Cladding temperature increasing and exposed in air
- Hydrides are already existing in the spent fuel cladding
  - 100ppm~1000ppm H in the cladding according to the burnup levels
  - Hydrogen effect is investigated under solution state at 650℃
    - Kearns' eq for hydrogen solubility in Zircaloy is 1134 ppm at 650℃

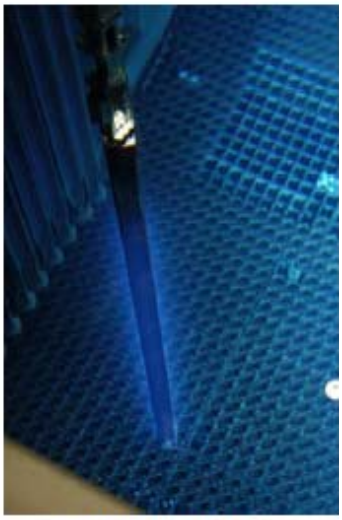

Spent fuel pool

Experimental

- Specimen hydriding
  - As-received Zircaloy-4 cladding tube was hydrogen-charged by a gaseously thermal cycling process
  - Target levels of 120 ppm H, 350ppm H, and 750 ppm H were obtained

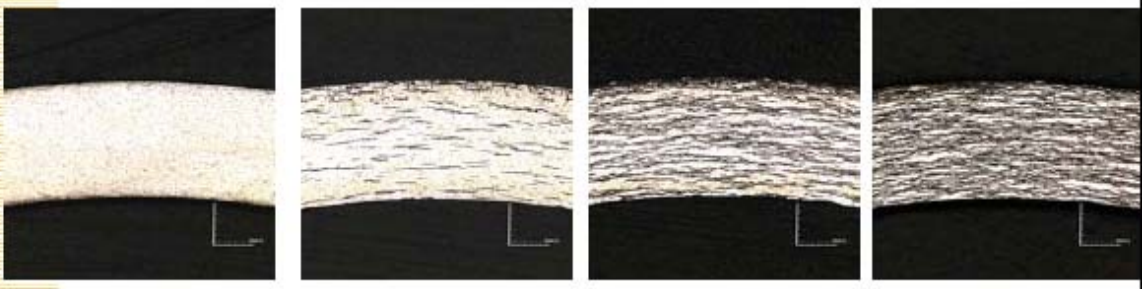

As-received | 120 ppm H | 350 ppm H | 750 ppm H

Experimental

- Oxidation test
  - SETARAM TGA：650℃ in air
  - Specimen condition:
    - ✓As-received Zr-4
    - ✓Zr-4 with 120ppm H
    - ✓Zr-4 with 350ppm H
    - ✓Zr-4 with 750ppm H

Specimen

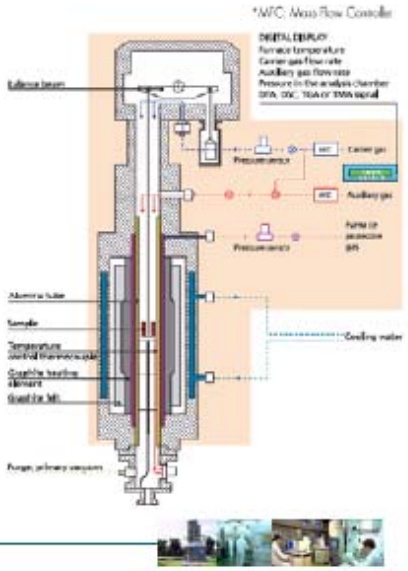

Results

- Hydrogen state in Zircaloy-4
  - Zr-4 with 750ppm H oxidation at 650℃ for 75 hours
  - Before oxidation：circumferential hydride strings
    - **ZrH_2 intermetallic compound**
  - After oxidation：hydride particles at grain boundary
    - **At 650℃, H in a state of solid solution**

Before oxidation

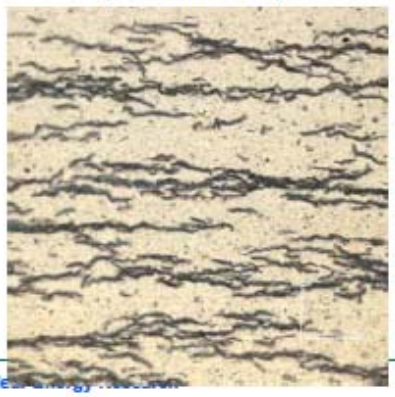

After oxidation

Results

- Oxidation kinetics
  - Transition of kinetics
  - Pre-transition
    - Parabolic rate
    - $W^2 = K_P \cdot t + C$
  - Post-transition
    - Linear rate
    - $W = K_L \cdot t + C$

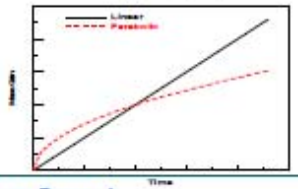

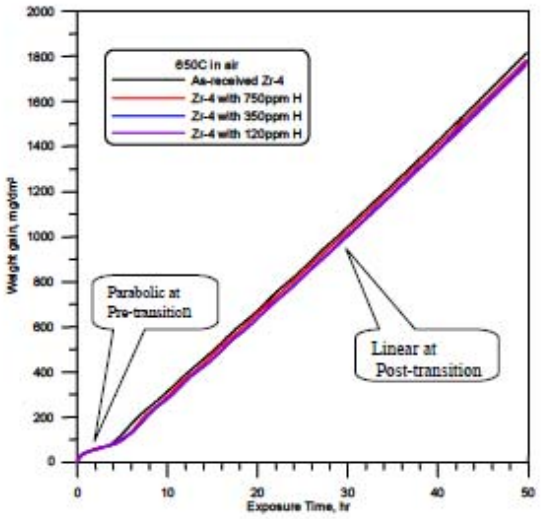

Results

- H effect on kinetics (before transition)
  - H increases the initial parabolic oxidation rate
  - Higher H content shows more rate increasement
  - H delays the occurrence of transition

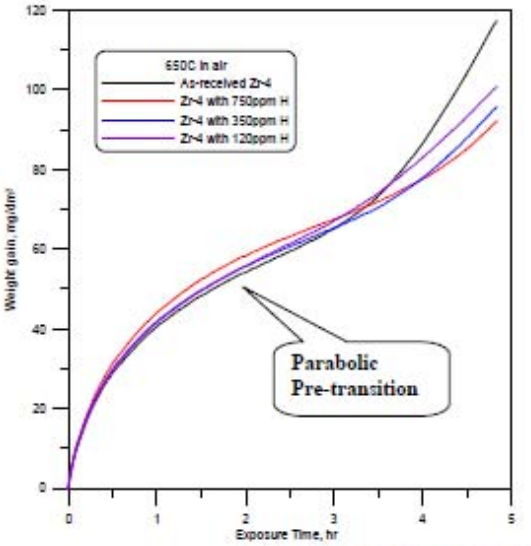

Results

- H effect on kinetics (after transition)
  - Hydrided specimens show lower weight gain in the linear regime
  - Lower H content shows more decrement

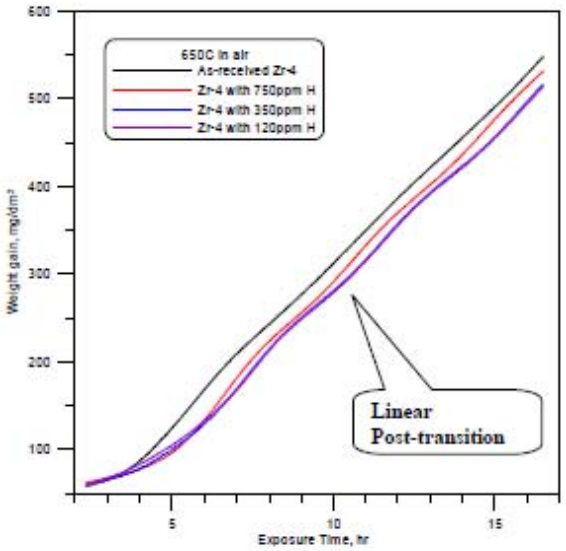

Results

- Structure of oxide
  - Pre-transition: few dis-continuous cracks
    - Protective scale for oxidation: parabolic rate
  - Post-transition: high density of continuous cracks
    - Loose and non-protective oxide layer: linear rate

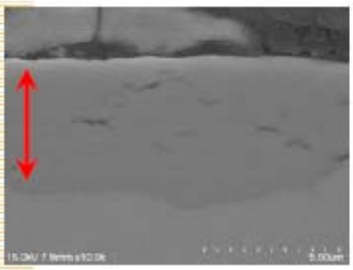

650℃ 1h ~5 μm

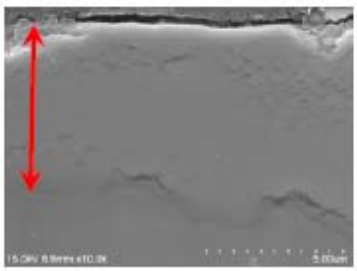

650℃ 2h ~6.5 μm

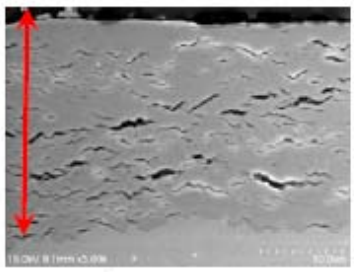

650℃ 10h ~25 μm

Conclusions

- Air oxidation of Zircaloy-4 cladding exhibits a transition of kinetics; parabolic rate law is shown in the pre-transition while linear rate law is revealed in the post-transition.
- Solution state of H in Zircaloy-4 cladding enhances the oxidation rate before transition; but hydrogen shows the effect of reducing the weight gain in the linear regime.
- H delays the occurrence of transition of oxidation kinetic.
- Only few dis-continuous cracks are seen in the oxide of pre-transition, while high density of continuous cracks are shown in the oxide of post-transition.

Thank you!